ELSEVIER

International Journal of Heat and Fluid Flow 19 (1998) 661–671

International Journal of HEAT AND FLUID FLOW

Flow boiling heat transfer on a heating element restricted by an interference sleeve

S. Madhusudana Rao, A.R. Balakrishnan *

Department of Chemical Engineering, Indian Institute of Technology Madras, Chennai 600 036, India

Received 1 May 1997; accepted 7 April 1998

Abstract

The flow boiling phenomenon over a heated tube restricted by an interference sleeve, which is a passive enhancement technique, has been analysed using a semi-empirical approach. The liquid boiled was water flowing through an annular cross-section. A model developed earlier for the case of pool boiling over porous surfaces has been adapted after modification to pool boiling with interference surfaces using equivalent geometrical parameters and a modified permeability factor. This was further extended to saturated flow boiling situation using an additive mechanism. The single phase heat transfer coefficient required for the additive mechanism is obtained from an experimental correlation developed in the present study. The suppression factors evaluated for the eight sleeve geometries used in the present investigation are expressed in terms of the single phase Reynolds number and the Martinelli parameter. Very good agreement was observed between the model predictions and experimental data validating the mechanisms postulated. Further, a purely empirical correlation based on the present experimental data has been proposed to estimate the two-phase heat transfer coefficient. While the empirical correlation shows a better fit with the experimental data, the additive model has a physical basis.

Notation

Bo	boiling number, (−)
Co	convective number, (−)
C_p	specific heat, J/(kg K)
d	pore diameter of the porous surface; hole diameter in the interference surface, m
d_b	departure diameter of the bubble, m
d_p	particle diameter of porous surface; equivalent diameter in the interference surface, m
D_{equ}	equivalent diameter of annular section ($=D_o - D_i$), m
D_i	diameter of inner tube of annulus, m
D_o	diameter of outer tube of annulus, m
Fr_l	Froude number, (−)
G	mass velocity of the liquid, kg/(m^2 s)
g	acceleration due to gravity, m/s^2
h	heat transfer coefficient, W/(m^2 K)
Ja	Jakob number $(\rho_l C_{pl}\Delta T_s)/(\rho_v \lambda)$
k	thermal conductivity, W/(m K)
$\dot{m}$	vapour mass flow rate, kg/s
N/A	active pore site density in porous surfaces; hole site density in interference surfaces, m^{-2}
p	hole pitch, m
Pr	Prandtl number $(C_p\mu/k)$, (−)
q	heat flux, W/m^2
Re	Reynolds number, (−)
S	suppression factor, (−)
T	temperature, K
ΔT_e	effective wall superheat, K
ΔT_s	wall superheat ($=T_w - T_s$), K
t	thickness of the interference surface, m
u_D	Darcy velocity, m/s
W_f	wetting factor, (−)
x	vapour quality, (−)
X_{tt}	Martinelli parameter, (−)

Greek

δ	clearance between the interference surface/sleeve and the heating element; δ_p: thickness of the porous matrix, m
ϵ	porosity of the porous matrix; fractional free area of the interference sleeve, (−)
κ	permeability of the porous matrix; κ_m: modified permeability for interference sleeves, (−)
λ	latent heat of vaporisation, J/kg
μ	viscosity, kg/(m s)
Ω	sleeve factor, (−)

Subscripts

l	large; liquid
p	porous
s	small; saturated
tp	two-phase
v	vapour
w	wall

* Corresponding author.

0142-727X/98/$ – see front matter
PII: S0142-727X(98)10033-4

1. Introduction

The use of porous surfaces is an important enhancement technique in flow boiling, though the mechanisms by which this phase change heat transfer takes place are not completely understood. Experimental results reported by Czikk et al. (1981) explain to some extent the effect of mass velocity on the boiling heat transfer coefficients. Their results showed that the mass velocity greatly affects the boiling heat transfer coefficient for oxygen boiling inside a horizontal tube that contained a porous coated surface.

An experimental study on pool boiling of water by Shimada et al. (1991) showed that an interference plate (a plate with small holes located on a specified pitch) placed with a small clearance over a flat copper heating surface traps the vapour bubbles stably and acts as a heat transfer enhancement technique. A salient feature of this arrangement is that its performance is comparable or better than the commercially available high performance boiling heat transfer surfaces evaluated by Gottzmann et al. (1973), and Ito et al. (1982, 1983). The interference plate used in this study was made of 6 mm thick polycarbonate sheet with varying hole geometries (size and pitch) and clearances above the heated surface. The primary advantage of using an interference plate over a boiling surface as a heat transfer enhancement technique over other enhancement techniques is the easy cleaning of fouling deposits. Secondly, preparation of the enhanced surface does not need sophisticated mechanical processing methods. The boiling mechanism on the heating surface with such interference surface over it is believed to be similar to that on a porous surface. In order to confirm this, an earlier model of pool boiling over porous surfaces by Rao and Balakrishnan (1997a) is extended to pool boiling over interference sleeves and then extended to flow boiling. The model is validated with experimental results obtained in the present study for flow boiling over a horizontal heated stainless steel tube which is restricted by an interference sleeve with holes.

2. Pool boiling over porous surfaces

O'Neill et al. (1972) developed a model to predict the heat flux in pool boiling over porous surfaces. The model consists of a term for the liquid film thickness expressed in terms of a geometrical parameter. This geometrical parameter depends on the particle packing geometry. The geometric parameters required for this model are evaluated for regular packings and are indeterminate for actual packings. Nakayama et al. (1980a, b) developed a semi-empirical additive model for the Thermoexcel E type surface – a commercial high performance surface consisting of pores with interconnecting tunnels below in a regular pattern. Their experimental results showed that the contribution of the heat flux due to single phase external convection was negligible compared to the latent heat flux contribution. Their model consisted of seven empirical constants which have to be evaluated for each surface–liquid combination. Kovalev et al. (1987, 1990) mathematically modelled the boiling behaviour by using the momentum and energy equations separately for both the liquid and vapour phases. These equations were solved numerically. This model is not easy to use (Webb, 1994). Rao and Balakrishnan (1997a, b) developed a model for pool boiling over porous surfaces by considering the pressure drop across the porous matrix. A brief description of this model is given in Appendix A. The total heat flux 'q' was expressed in terms of the wall superheat, physical properties of the boiling fluid and the geometry of the porous matrix. The final expression for the heat flux was given by

$$q = 2.4 \times 10^{-4} \frac{\rho_l \rho_v^2 k \lambda^2 \, \Delta T_s (\delta_p/d)^{0.8} \mathrm{Ja}^{0.22}}{\mu_v \delta_p T_s (\rho_l - \rho_v) \epsilon^{1.23}}. \quad (1)$$

3. Extension to pool boiling over interference sleeves

The model developed for pool boiling over porous surfaces can be extended to pool boiling over surfaces restricted by an interference plate with holes by appropriately defining the different geometrical parameters. The following considerations are involved in the development of this extension:

1. The vapour liquid exchange mechanism is the same for both porous surfaces and interference surfaces.
2. Extension of the model for porous surfaces to interference plates or sleeves requires modification of the permeability factor. The fraction of the free area of the interference plate or sleeve is considered equivalent to the porosity of the porous matrix.
3. Since the vapour is generated from the base surface with interference plates, the assumption of constant matrix temperature of the porous surfaces is valid here also.

Shimada et al. (1991) studied two types of hole geometries on a triangular pitch, namely, holes with a uniform diameter and holes with a combination of two diameters as shown in Fig. 1. From Fig. 1(a) it may be seen that the fractional free area, which is equivalent to the porosity in a porous matrix, can be expressed as

$$\epsilon = 0.91(d^2/p^2). \quad (2)$$

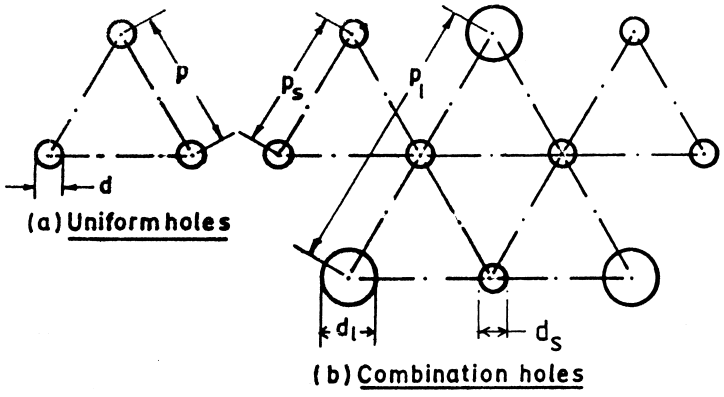

Fig. 1. Hole geometries with triangular pitch: (a) uniform holes; (b) combination holes.

For combination holes, ϵ can be written as (see Fig. 1(b))

$$\epsilon = 0.52\left(\frac{d_l^2 + 2d_s^2}{p_l p_s}\right). \tag{3}$$

Shimada et al. (1991) reported heat transfer data for pool boiling of water for a large number of interference plate geometries. The pitch of the holes were varied from 4×10^{-3} to 14×10^{-3} m, the hole diameter from 1×10^{-3} m to 8×10^{-3} m and the gap clearance between the interference plate and the heating surface from 5×10^{-5} m to 3×10^{-3} m. The model for pool boiling on porous surfaces is compared with the data of Shimada et al. (1991). In order to do this, the porosity of the matrix, ϵ, has to be substituted with the fractional free area as defined by Eqs. (2) and (3) above. The permeability 'κ' is adjusted to match the data and the model. A correction factor is then applied to the permeability obtained by the straight tube model (see Appendix A) to match the adjusted or modified permeability, so that

$$\kappa_m = C_1 \cdot \left(\frac{\epsilon d^2}{32}\right). \tag{4}$$

The correction factor is correlated with the geometry of the sleeve as

$$C_1 = 6.92 \times 10^{-3}\left(\frac{\delta}{d_b}\right)^{-0.52}. \tag{5}$$

In the above expression 'd_b' is the bubble departure diameter from a plain surface and 'δ' is the gap clearance between the heating element and the interference plate. The bubble departure diameter d_b can be estimated using the expression due to Cole and Rohsenow (1969) and is

$$d_b = C_2\left(\frac{\sigma}{g(\rho_l - \rho_v)}\right)^{1/2}(\mathrm{Ja}^*)^{5/4}, \tag{6}$$

where $C_2 = 1.5 \times 10^{-4}$ for water and Ja^* is the modified Jakob number defined as

$$\mathrm{Ja}^* = \frac{\rho_l C_{p_l} T_s}{\rho_v \lambda}. \tag{7}$$

An expression for the pool boiling heat transfer coefficient with interference plates can be obtained by rearranging Eq. (1) (using the modified permeability κ_m as defined by Eq. (4) above) and is

$$h_{pool} = 2.4 \times 10^{-4} \times \frac{\rho_l^{1.22} C_{p_l}^{0.22} \rho_v^{1.78} \kappa_m \lambda^{1.78} (\Delta T_s)^{0.22} (t/d)^{0.8}}{\mu_v t T_s (\rho_l - \rho_v) \epsilon^{1.23}}. \tag{8}$$

4. Extension to flow boiling over interference surfaces

When a flow situation exists on a heating surface which is restricted by an interference plate/sleeve, the moving liquid sweeps or takes away the vapour bubbles emerging out of the holes. Hence, the expected bubble departure diameters would be smaller with flow boiling. Chen (1966) explained that the existence of high two-phase Reynolds numbers associated with significant vapour qualities results in nucleation suppression.

As may be seen from the illustration in Fig. 2, whether in pool boiling or flow boiling, the degree of superheat is not constant across the boundary layer. The convective effects associated with pool boiling are small, so the difference between the effective superheat ΔT_e and ΔT_s can be neglected. However, this difference is not negligible in the case of flow boiling. The liquid temperature gradient for flow boiling depends on the flow rate and vapour quality and in general will be much steeper than in the corresponding pool boiling case

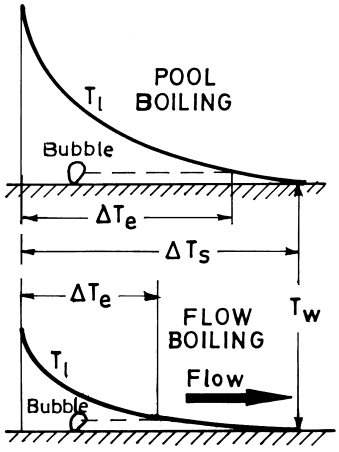

Fig. 2. Temperature profiles in pool boiling and in flow boiling at a given wall superheat.

for the same wall superheat. Eq. (8) for pool boiling was developed by assuming that the external convective effects were negligible and therefore the wall superheat and the effective superheat were the same. Eq. (8) is hence modified to take into account the convective effects using the effective superheat to represent the nucleate heat transfer coefficient and is given by

$$h_{nuc} = 2.4 \times 10^{-4} \times \frac{\rho_l^{1.22} C_{p_l}^{0.22} \rho_v^{1.78} \kappa_m \lambda^{1.78} (\Delta T_e)^{0.22} (t/d)^{0.8}}{\mu_v t T_s (\rho_l - \rho_v) \epsilon^{1.23}}. \tag{9}$$

Furthermore, in the present study a suppression factor, S, is defined as the ratio of the effective to true wall superheat at the wall

$$S = \left(\frac{\Delta T_e}{\Delta T_s}\right)^{0.22}. \tag{10}$$

Combining Eqs. (9) and (10), the nucleate boiling heat transfer coefficient in terms of this suppression factor is given by

$$h_{nuc} = 2.4 \times 10^{-4} \times \frac{\rho_l^{1.22} C_{p_l}^{0.22} \rho_v^{1.78} \kappa_m \lambda^{1.78} (\Delta T_s)^{0.22} (t/d)^{0.8}}{\mu_v t T_s (\rho_l - \rho_v) \epsilon^{1.23}} \cdot S. \tag{11}$$

Unlike in pool boiling the additive mechanism has a significant role in convective boiling. The single phase heat transfer coefficient cannot be neglected when the convective Reynolds numbers are high. Therefore, the total heat transfer coefficient for convective boiling is

$$h = h_{nuc} + h_{con}. \tag{12}$$

However, the single phase heat transfer coefficient cannot be estimated using conventional correlations when the flow is over the interference surface/sleeve. In the present study, single phase heat transfer data was obtained on a heated cylinder restricted by interference sleeves. The test liquid was water flowing over the interference sleeves in an annular section.

5. Experimental

A schematic of the experimental set-up is shown in Fig. 3. The test loop consists of a horizontal test section, a separator or water storage tank, a preheater, an orificemeter connected to an inclined tube manometer and a water cooled glass condenser. Fig. 4 shows the details of the test section which consists essentially of a horizontal heated stainless steel tube. The

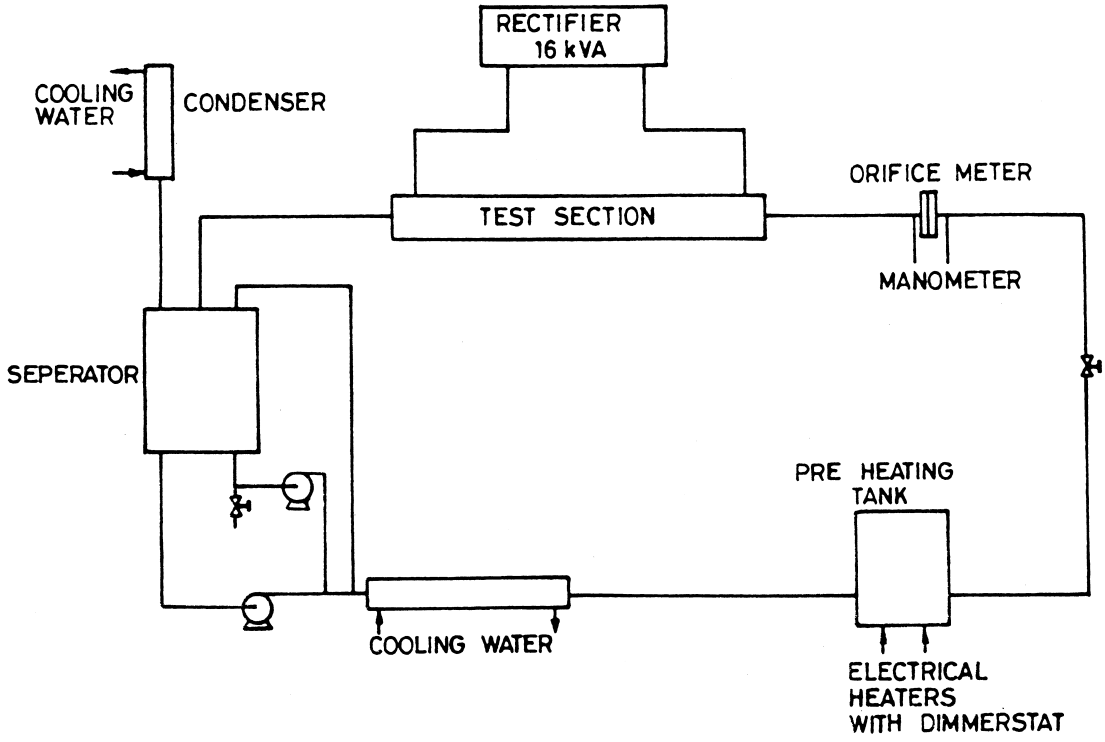

Fig. 3. Schematic layout of the experimental set-up.

stainless tube in concentrically placed in a glass pipe so that boiling which takes place on the outside of the heated stainless tube can be visually observed when water flows axially in the annular space between the heated stainless tube and the outer glass pipe. The stainless steel tube is heated with a DC power supply using a 16 kVA rectifier with copper terminals and a bus-bar arrangement. Power input is varied using a step-up/step-down arrangement in the rectifier and the corresponding wall temperatures are recorded using thermocouples imbedded in the tube walls. Power input is estimated from the product of the voltmeter and ammeter readings of the rectifier. Chromel–alumel thermocouple wires (24 gauge) were used for temperature measurements. Three thermocouple wires are fixed at 90° intervals around the circumference of the heated tube wall to which they are silver soldered with metal studs. The average of these three thermocouple readings gives the mean wall temperature of the heating surface 'T_w'. The digital millivoltmeter used to measure the emf generated by the thermocouple wires has a resolution of 0.01 mV. Mass velocity of the water entering the test section is measured by the calibrated orifice-meter with an inclined tube mercury manometer. Inlet temperature of water is maintained at saturation temperature using a pre-heater with dimmerstat control. The water outlet of the test section is exposed to the atmosphere. The quality of

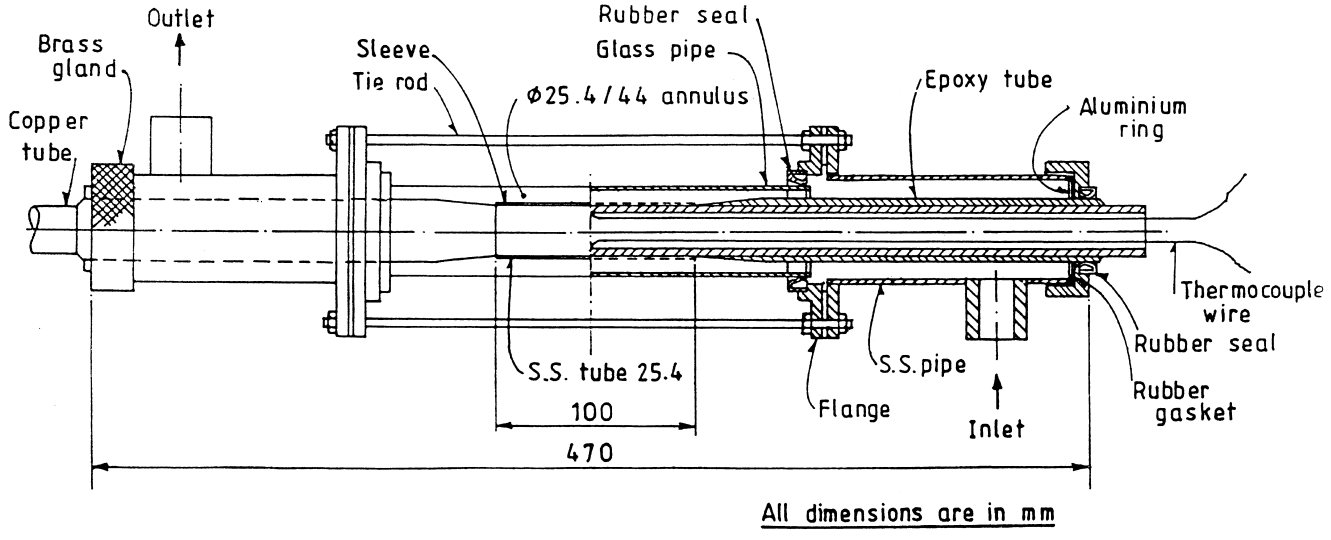

Fig. 4. Test section details.

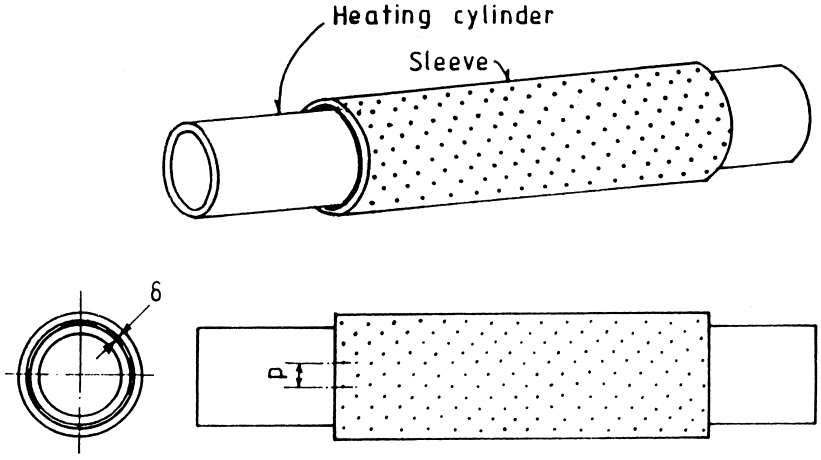

Fig. 5. Arrangement of the sleeves over the heating cylinder.

the vapour is estimated by performing an energy balance. Necessary precautions are taken to ensure degassing and ageing of the heated surface.

The arrangement of the interference sleeves over the stainless steel tube is shown in Fig. 5. Uniform clearance between the heating tube and the sleeve is ensured by using Teflon rings. The performance of a much large tube with sleeve is simulated by sealing the ends, so that liquid/vapour can reach/leave the tube only through the holes and not through the gap clearance. A total of eight sleeves were used with different hole geometries and gap clearances. These details are summarized in Table 1. Mass velocities were varied from 577 to 1347 kg/(m^2 s). The flow in the annulus was in the turbulent regime.

6. Results and discussion

The single phase heat transfer data over the sleeves has been correlated as

$$\mathrm{Nu}_{\mathrm{con}} = \frac{\mathrm{Re}_{\mathrm{l}}^{0.4}}{\mathrm{Pr}_{\mathrm{l}}^{0.73}}, \tag{13}$$

where $\mathrm{Nu}_{\mathrm{con}} = (h_{\mathrm{con}} D_{\mathrm{eq}})/k_{\mathrm{l}}$ $\mathrm{Re}_{\mathrm{l}} = (GD_{\mathrm{eq}})/\mu_{\mathrm{l}}$, $\mathrm{Pr}_{\mathrm{l}} = (C_{\mathrm{p_l}}\mu_{\ell})/k_{\mathrm{l}}$. The performance of the correlation is shown in Fig. 6.

Boiling data obtained with these eight sleeves were used to evaluate the suppression factors from Eqs. (11)–(13). These suppression factors are expressed in terms of the liquid phase Reynolds number and the well known Martinelli parameter which is representative of vapour quality. Unfortunately, it was not possible to obtain a unique expression for the suppression factor for all eight sleeves. The individual expressions are given in Table 2. Although the number of data points for each expression is limited, the fit was extremely good with a variation of less than ±3%. It is for this reason that attempts to obtain a unique expression for all eight sleeves were not pursued. The Martinelli parameter, X_{tt}, used in the expressions in Table 2 is defined by

$$X_{\mathrm{tt}} = \left(\frac{\rho_{\mathrm{v}}}{\rho_{\mathrm{l}}}\right)^{0.5}\left(\frac{\mu_{\mathrm{l}}}{\mu_{\mathrm{v}}}\right)^{0.1}\left(\frac{1-x}{x}\right)^{0.9}. \tag{14}$$

The range of Reynolds numbers used in developing the above expressions given in Table 2 is 3.7×10^4 to 8.62×10^4. Fig. 7(a)–(h) show the comparison of the model with the experimental data obtained in the present study for all the eight sleeve geometries considered at different inlet liquid mass velocities. Good agreement may be seen between the model predictions and the experimental data. Suppression factors obtained with the eight sleeves at three mass velocities is shown in Fig. 8(a)–(c).

Chen (1966) proposed the nucleation suppression concept by considering the two-phase Reynolds numbers when the vapour qualities are significant. But, in the present study, despite low vapour qualities, the nucleation suppression factors are high. The present data is obtained for water boiling at atmospheric pressure. The vapour void fractions correspond-

Table 1
Sleeve geometries used in the present study

Sleeve no.	Hole diameter d, mm	Pitch p, mm	Clearance δ, mm	Wall thickness t, mm	No. of holes per m^2
1	1	4	0.36	2.78	8.8×10^4
2	1	8.3	0.36	2.78	2.0×10^4
3	1	14.3	0.36	2.78	7.0×10^3
4	1,2 (combination)	4,8 (combination)	0.36	2.78	5.8×10^4 2.7×10^4
5	1	4	0.92	3.58	9.1×10^4
6	1	4	2.3	2.25	9.1×10^4
7	1,2 (combination)	14.3, 24.8 (combination)	0.36	2.78	4.5×10^3 1.6×10^3
8	2	4	0.36	2.78	8.8×10^4

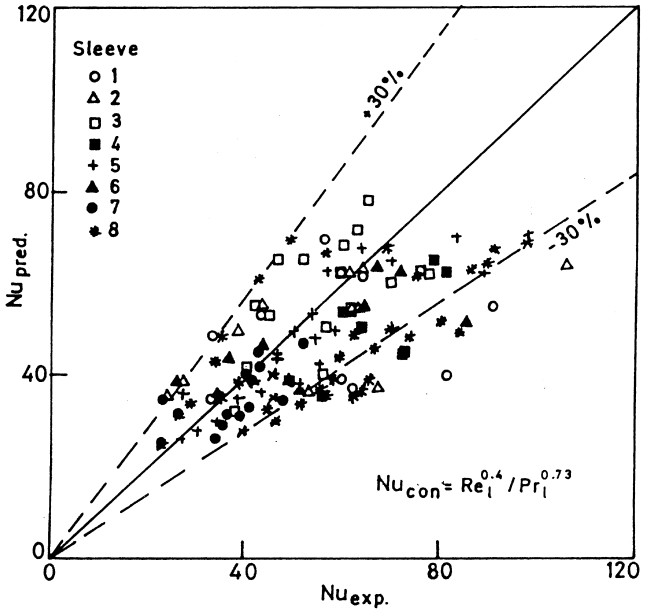

Fig. 6. Performance of the correlation for convective heat transfer with interference sleeves.

ing to the vapour qualities can be estimated using the correlation proposed by Rouhani (1969)

$$\sigma_v = \frac{x}{\rho_v}\left[[1+0.12(1-x)]\left(\frac{x}{\rho_v}+\frac{1-x}{\rho_l}\right) + \frac{1.18(1-x)[g\sigma(\rho_l-\rho_v)]^{0.25}}{G\rho_l^{0.5}}\right]^{-1}. \quad (15)$$

The estimated void fractions for sleeve 1 and the plain tube without sleeve are shown in Fig. 9(a)–(c) for three different inlet liquid mass velocities, namely, 577, 962 and 1347 kg/(m^2 s), respectively. It may be noted that the void fraction values are significant. At any given wall superheat sleeves show higher heat flux values than plain tubes. This results in the generation of more vapour and therefore larger void fractions result. Visual observations indicate that the test section is either in bubbling mode or in the slug mode when heat fluxes are low and the mass velocities are high. On the other hand, at high heat flux conditions the upper portion of the test section could get filled with vapour and this could result in flow separation, thereby effecting a shift from the bubbling or slugging regime to the stratified regime. Similarly, low mass velocities and moderate heat fluxes also could result in flow separation. This could be the reason for significant suppression factors even at low vapour qualities. Furthermore, it may also be noted that the wall superheats are low with sleeve 1 when compared to a plain tube without sleeves at the same void fractions. In developing the present model, the coalescence of the bubbles in the clearance gap between the sleeve and the heating cylinder was not considered. This could be a reason for some deviation between the model and the experimental data with sleeves with higher pitch as may be seen in Fig. 7(c). When sleeves with large values of pitch are used, the vapour in the gap clearance (the clearance between the heating cylinder and the sleeve) has to travel a large distance along the heating surface before discharging from a nearby hole. This causes coalescence of the bubbles which give rise to higher heat transfer coefficients. This phenomena was also observed experimentally in a parallel study on sub-cooled flow boiling over interference sleeves by Rao and Balakrishnan (1997b). They further reported that the use of interference sleeves gave enhancement factors (defined as the ratio of the wall superheats without and with sleeves at the same heat flux) of up to 2, at a mass velocity of 478 kg/(m^2 s) and an inlet sub-cooling of 5 K. Rao (1997) has shown that under saturated boiling conditions even higher enhancements can be achieved. For example, at a mass velocity of 962 kg/(m^2 s), enhancement factors as high as 8 were observed using sleeve 3. Unfortunately, high enhancement factors were reported to be accompanied by an early transition to film boiling. This appears to point towards bubble coalescence, alluded to earlier.

6.1. Empirical correlation

The saturated boiling data obtained in the present study has been analysed following the approach of Shah (1982) and an empirical correlation proposed to estimate the two-phase heat transfer coefficient in the nucleate boiling regime. The correlation is

$$\psi = 46.54\left(\frac{1}{W_f}\right)^{0.21} \cdot \Omega. \quad (16)$$

Ω is the sleeve factor that depends on the geometry of the holes in the sleeve and is given by

$$\Omega = \frac{1}{\epsilon^{0.23}}\left(\frac{\delta}{d}\right)^{0.1} \quad (17)$$

Table 2
Suppression factors for various sleeves used in the present study

Sleeve no.	Expression for suppression factor	Martinelli parameter range (X_{tt})	No. of data points	Standard deviation
1	$S = 136/X_{tt}^{0.87}Re_l^{0.34}$	$13.6 \leqslant X_{tt} \leqslant 163.8$	13	13.14
2	$S = 11.6/X_{tt}^{1.1}Re_l^{0.1}$	$21.5 \leqslant X_{tt} \leqslant 156.4$	11	20.5
3	$S = 6.18 \times 10^4/X_{tt}^{0.64}Re_l^{0.88}$	$38.6 \leqslant X_{tt} \leqslant 122.6$	9	40.5
4	$S = 71.36/X_{tt}^{0.24}Re_l^{0.49}$	$10.3 \leqslant X_{tt} \leqslant 175$	16	19.5
5	$S = 5 \times 10^8/X_{tt}^{0.12}Re_l^{1.87}$	$12.8 \leqslant X_{tt} \leqslant 171.1$	12	33.1
6	$S = 9 \times 10^5/X_{tt}^{0.8}Re_l^{1.25}$	$18.2 \leqslant X_{tt} \leqslant 135.7$	9	19.0
7	$S = 6.26 \times 10^6/X_{tt}^{0.37}Re_l^{1.5}$	$23 \leqslant X_{tt} \leqslant 171.1$	9	21.1
8	$S = 0.36/X_{tt}^{0.15}Re_l^{0.11}$	$8.2 \leqslant X_{tt} \leqslant 168.1$	18	18.2

Note: The Re_l range in the above expressions was 3.7×10^4–8.62×10^4.

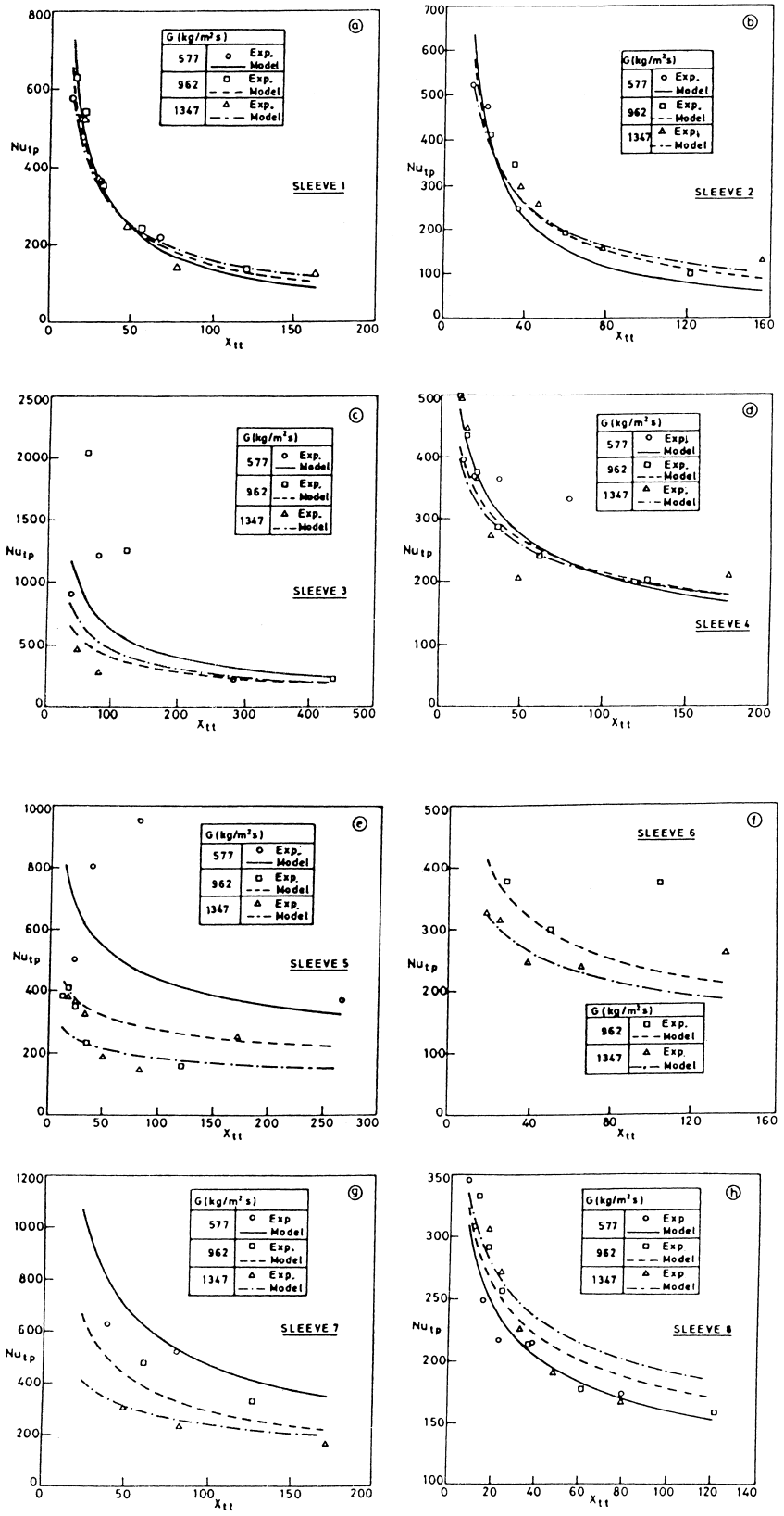

Fig. 7. Comparison of model predictions with experimental data: (a) Sleeve 1 with 4 mm hole pitch, 1 mm hole diameter and 0.36 mm clearance; (b) Sleeve 2 with 8.3 mm hole pitch, 1 mm hole diameter and 0.36 mm clearance; (c) Sleeve 3 with 14.3 mm hole pitch, 1 mm hole diameter and 0.36 mm clearance; (d) Sleeve 4 with combination holes of 1 and 2 mm diameter on 4 and 8 mm hole pitch, respectively and 0.36 mm clearance; (e) Sleeve 5 with 4 mm hole pitch, 1 mm hole diameter and 0.92 mm clearance; (f) Sleeve 6 with 4 mm hole pitch, 1 mm hole diameter and 2.3 mm clearance; (g) Sleeve 7 with combination holes of 1 and 2 mm on 14.3 and 24.8 mm hole pitch, respectively and 0.36 mm clearance; (h) Sleeve 8 with 4 mm hole pitch, 2 mm hole diameter and 0.36 mm clearance.

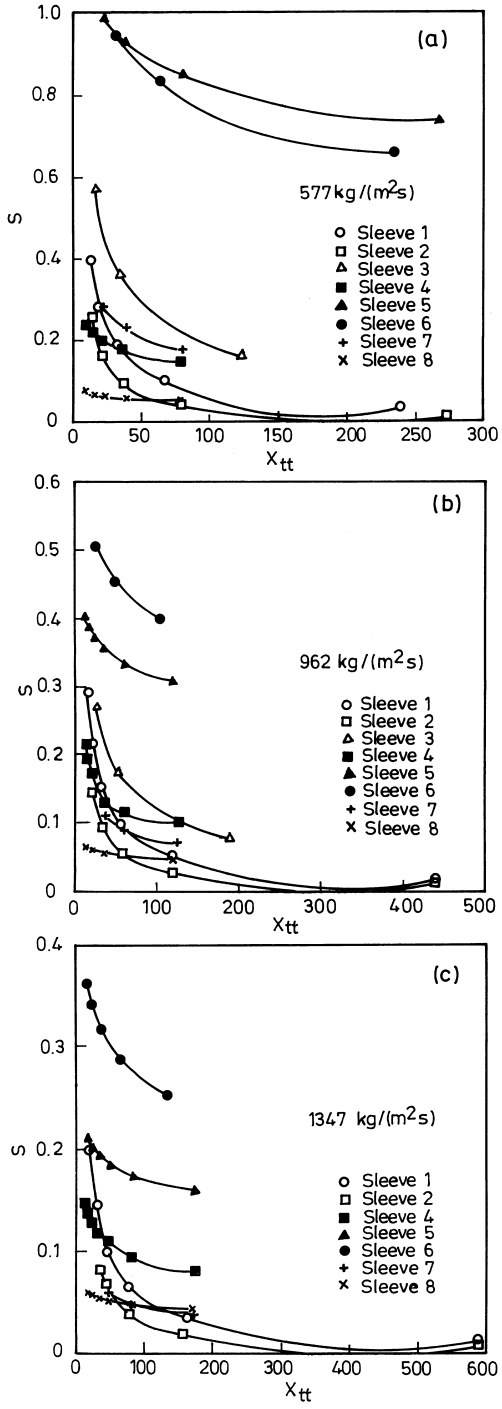

Fig. 8. Suppression factors of the eight sleeves used in the present investigation using the additive model: (a) $G = 577$ kg/(m^2 s); (b) $G = 962$ kg/(m^2 s); (c) $G = 1347$ kg/(m^2 s).

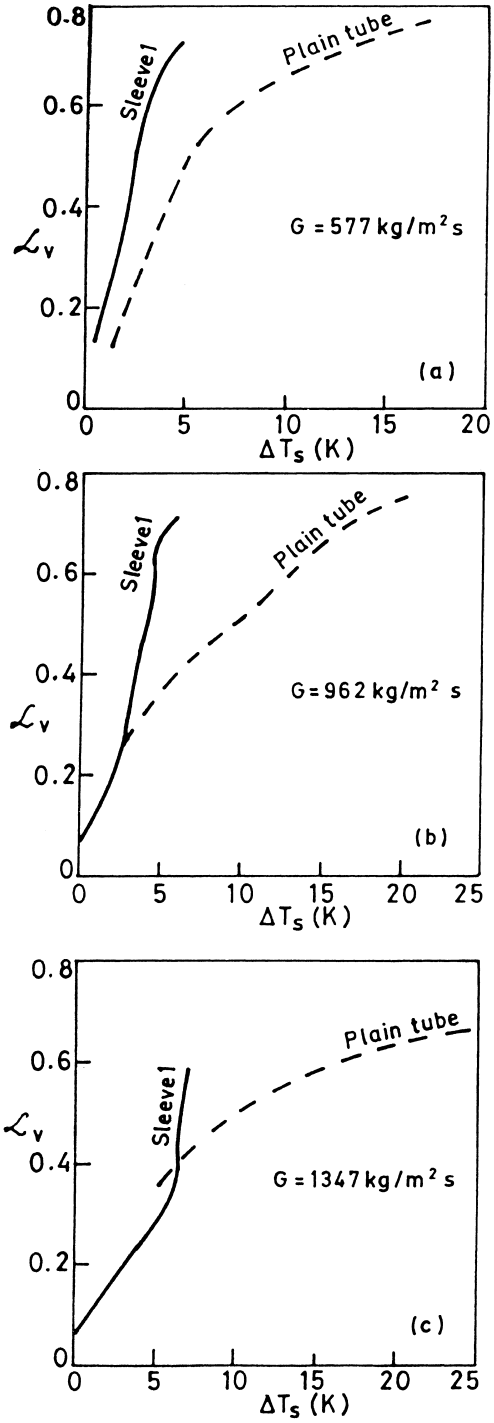

Fig. 9. Comparison of the estimated void fractions for sleeve 4 and plain tube: (a) $G = 577$ kg/(m^2 s); (b) $G = 962$ kg/(m^2 s) and (c) $G = 1347$ kg/(m^2 s).

and ψ is the ratio of the two-phase or boiling heat transfer coefficient to the forced convection or single phase heat transfer coefficient over sleeves

$$\psi = \frac{h_{tp}}{h_l}, \tag{18}$$

where h_l can be determined from Eq. (13).

W_f is a wetting factor defined as the ratio of the Froude number and the boiling number

$$W_f = \mathrm{Fr}_l/\mathrm{Bo},$$

where

$$\mathrm{Fr}_l = G^2/(\rho_l^2 g D_{eq}),$$

$$\mathrm{Bo} = q/(G\lambda).$$

The range of variables covered in the present study are

$2 \times 10^{-6} < \mathrm{Bo} < 1.5 \times 10^{-4}; \quad 2 < \mathrm{Co} < 70;$
$2 < \mathrm{Fr_l} < 11.$

Co is the convective number and is defined by

$$\mathrm{Co} = \left(\frac{1-x}{x}\right)^{0.8}\left(\frac{\rho_v}{\rho_l}\right)^{0.5}. \tag{19}$$

In the present study, the Convection number is always greater than one. According to Shah (1982), Co > 1 implies the nucleate boiling regime where ψ is independent of Co and depends only on the Boiling number. Furthermore, according to Shah (1982), the two-phase convective effects in this regime are negligible and heat transfer enhancement is determined solely by the intensity of bubble nucleation. However, the data obtained in the present study shows that ψ is dependent on the Froude number in addition to the boiling number indicating that the convective effects are indeed important. Furthermore, in spite of low vapour qualities encountered, the large local void fractions encountered in the narrow confines of the annular geometry cause suppression of nucleation. W_f, the wetting factor, accounts for such local nucleation suppression effects. At low liquid mass velocities the Froude numbers are low and the channel is likely to be in the stratified flow regime. This gives low W_f values and hence high two-phase heat transfer coefficients. Moreover, at the same liquid mass velocity but with higher heat flux, the boiling number is high giving rise to a low W_f value again leading to high two-phase heat transfer coefficients. So it is seen that W_f reflects the effect of both liquid inlet mass velocity and the applied heat flux. The performance of the correlation is shown in Fig. 10. The standard deviation of the data is 19.67%. The total number of data points in the figure is 73 and the agreement between the correlation and the data is within ±30%.

Fig. 11 shows a comparison of the experimental data with both the additive model described earlier and the empirical correlation. It can be seen that both the approaches are satisfactory, in that both match the data. However, the additive model has a physical basis using as it does Chen's (Chen, 1966) suppression concept, while the latter uses the boiling number

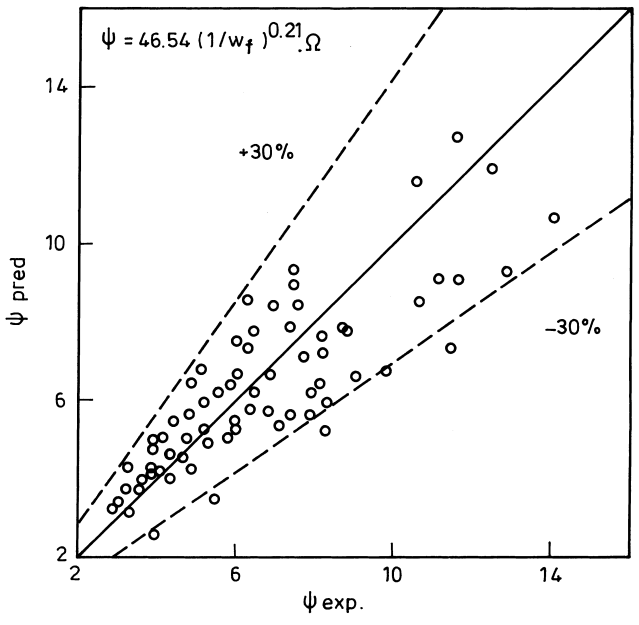

Fig. 10. Performance of the empirical correlation for flow boiling over interference sleeves.

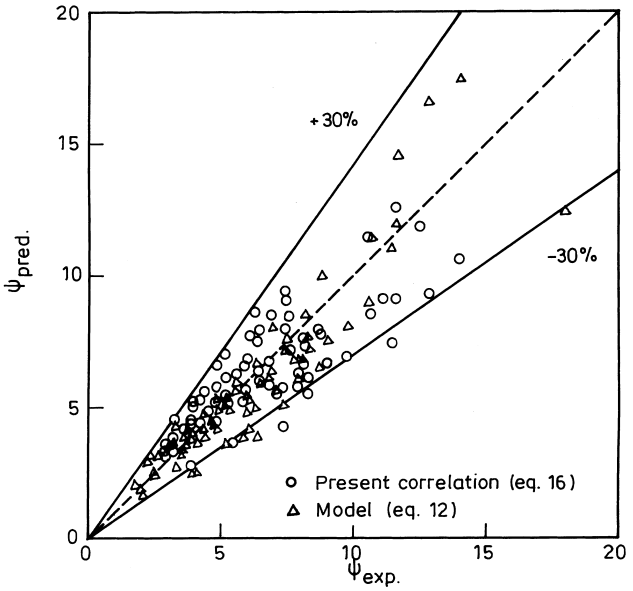

Fig. 11. Comparison of the experimental data with predicted values from the model and the empirical correlation.

empirically. The model requires separate expressions for the suppression factor for each sleeve while an appropriately defined common sleeve factor is satisfactory for all the sleeves in the correlation.

The data obtained in the present study are either in the bubbling mode or in the slugging mode. The annular stratified conditions are observed only at high heat flux conditions and at low mass velocities. The wall superheats reported in this investigation are the mean of the local values taken circumferentially. W_f, defined as the wetting factor, incorporates the boiling suppression effects. The correlations for flow boiling through tubes based on the boiling number (e.g. Shah, 1982) are generally given in terms of the ratio of the two-phase heat transfer coefficient and the single phase heat transfer coefficient as a function of either the boiling number or the Froude number. Different correlations are available in the literature, depending on the boiling number and the Froude number. The term W_f is a unified parameter which accounts for both the flow and the applied heat flux. In the additive model these effects are treated separately.

Uncertainty in measurements: The resolution of the temperature measurement is 0.2°C. The power input is estimated from the product of the voltmeter and ammeter readings. The resolution of the voltmeter is 0.04 V and that of the ammeter is 10 A. The accuracy in measuring the liquid mass velocity is 10 kg/(m^2 s).

7. Conclusions

Flow boiling over a heated cylinder with an interference sleeve has been examined both analytically as well as experimentally. An additive model based on pool boiling over porous surfaces and incorporating nucleate boiling suppression in the flow boiling mode has been proposed and compared with experimental data. The experimental data has also been correlated empirically. The study shows that there is significant nucleate boiling suppression in spite of low qualities encountered, due primarily to the high void fractions in the narrow annular cross-section available for flow. The study further shows that both inlet liquid mass velocity and the applied heat

flux are important in the geometry used. Bubble coalescence is important in those sleeves that have large hole pitch and gap clearance.

Acknowledgements

This work is part of a study funded by the Department of Atomic Energy, Government of India through the Board of Research in Nuclear Sciences, Bhabha Atomic Research Centre, Mumbai, India.

Appendix A

Rao and Balakrishnan (1997a) analysed the pool boiling phenomena over porous surfaces. A small superheat initiates nucleation over the porous surface. The vapour formed in the pores starts moving up as more and more vapour accumulates inside the porous surface. The pressure drop across the porous layer that causes the upward movement of vapour can be estimated from Darcy's law

$$\frac{\mathrm{d}P}{\mathrm{d}y} = \frac{\mu_\mathrm{v}}{\kappa} u_\mathrm{D}. \tag{A.1}$$

Assuming the vapour in the porous medium is moving upwards through capillary tubes of diameter 'd' formed between spherical particles of uniform diameter 'd_p', the Darcy velocity 'u_D' can be written as

$$u_\mathrm{D} = \frac{\dot{m}}{\rho_\mathrm{v}(\pi d^2/4)}, \tag{A.2}$$

where $\dot{m}$ is the mass flow rate of the vapour through the porous layer and is given by

$$\dot{m} = \frac{q_\mathrm{l}}{\lambda(N/A)}. \tag{A.3}$$

In the above equation 'q_l' is the latent heat contribution of the total heat flux 'q' and (N/A) is the number of active pores per unit area. Substituting Eqs. (A.2) and (A.3) into Eq. (A.1) gives the pressure drop across the porous layer of thickness 'δ_p'

$$\Delta P = \frac{1.27 q_\mathrm{l} \delta_\mathrm{p} \mu_\mathrm{v}}{\rho_\mathrm{v} \lambda d^2 (N/A) \kappa}. \tag{A.4}$$

The permeability 'κ' can be estimated from the straight tube model reported by Kaviany (1991) and is given by

$$\kappa = \frac{\epsilon d^2}{32}. \tag{A.5}$$

Using the pressure drop from Eq. (A.4) in the well-known Clapeyron equation and rearranging, the latent heat flux can be expressed as

$$q_\mathrm{l} = \frac{\rho_\mathrm{l} \rho_\mathrm{v}^2 \kappa \lambda^2 d^2 \, \Delta T_\mathrm{s} (N/A)}{1.27 \mu_\mathrm{v} \delta_\mathrm{p} T_\mathrm{s} (\rho_\mathrm{l} - \rho_\mathrm{v})}. \tag{A.6}$$

The total heat flux 'q' is

$$q = q_\mathrm{l} + q_\mathrm{ex}, \tag{A.7}$$

where 'q_ex' is the contribution of the heat flux due to single phase convection over the porous surface and is evaluated using an expression due to Nakayama et al. (1980b)

$$q_\mathrm{ex} = \left(\frac{\Delta T_\mathrm{s}}{C_\mathrm{q}}\right)^{5/3} \left(\frac{N}{A}\right)^{1/3}. \tag{A.8}$$

'C_q' is an empirical constant which depends on the liquid being boiled. This model compared very well with the experimental results of Nakayama et al. (1980a) for the two surfaces reported by them. Their data was obtained on surfaces whose porosities were 0.013 and 0.02. Working on these surfaces Nakayama et al. (1980a) showed experimentally that the heat flux due to single phase convection is about 10% of the total heat flux. However porous coatings generally give rise to very high active pore density and hence it is believed that for highly porous surfaces the total heat flux consists mostly of latent heat flux and the convective contribution can be ignored. Using the data of Tehver et al. (1992) for boiling on porous surfaces under burnout conditions when all the pores are active, the nucleation site density was obtained as

$$\frac{N}{A} = 3 \times 10^{-4} \frac{(\delta_\mathrm{p}/d)^{0.8} \, \mathrm{Ja}^{0.22}}{\epsilon^{1.23} d^2}. \tag{A.9}$$

Substituting the above into Eq. (A.6), the total heat flux 'q' is given by

$$q = 2.4 \times 10^{-4} \frac{\rho_\mathrm{l} \rho_\mathrm{v}^2 \kappa \lambda^2 \, \Delta T_\mathrm{s} (\delta_\mathrm{p}/d)^{0.8} \, \mathrm{Ja}^{0.22}}{\mu_\mathrm{v} \delta_\mathrm{p} T_\mathrm{s} (\rho_\mathrm{l} - \rho_\mathrm{v}) \epsilon^{1.23}}. \tag{A.10}$$

References

Chen, J.C., 1966. Correlation for boiling heat transfer to saturated fluids in convective flow. Ind. Eng. Chem. Process Des. Dev. 5, 322–329.

Cole, R., Rohsenow, W.M., 1969. Correlation of bubble departure diameters for boiling of saturated liquids. Chem. Eng. Prog. Symp. Ser. 65, 211–213.

Czikk, A.M., O'Neill, P.S., Gottzmann, C.F., 1981. Nucleate boiling from porous metal films: Effect of primary variables. In: Webb, R.L., Carnavos, T.C., Hostetler, K.M. (Eds.), Advances in Enhanced Heat Transfer, vol. 18. HTD ASME, New York, pp. 109–122.

Gottzmann, C.F., O'Neill, P.S., Minton, P.E., 1973. High efficiency heat exchangers. Chem. Eng. Prog. 69, 69–75.

Ito, T., Nishikawa, K., Tanaka, K., 1982. Evaluation of potential high performance porous boiling surfaces. Trans. Jpn Assoc. Refrigeration 57, 25–29.

Ito, T., Nishikawa, K., Tanaka, K., 1983. Evaluation of potential high performance porous boiling surfaces. In: Proceedings of 20th National Heat Transfer Symposium, vol. B211, pp. 232–234.

Kaviany, M., 1991. Principles of Heat Transfer in Porous Media. Springer, New York.

Kovalev, S.A., Solovyev, S.L., Ovodkov, O.A., 1987. Liquid boiling on porous surfaces. Heat Transfer – Soviet Research 19, 109–120.

Kovalev, S.A., Solovyev, S.L., Ovodkov, O.A., 1990. Theory of boiling heat transfer on a capillary porous surface. In: Proceedings of Nineth International Heat Transfer Conference, vol. 2, pp. 105–110.

Nakayama, W., Daikoku, T., Kuwahara, H., Nakajima, Y., 1980a. Dynamic model of enhanced boiling heat transfer on porous surfaces – Part I. ASME Journal of Heat Transfer 102, 445–450.

Nakayama, W., Daikoku, T., Kuwahara, H., Nakajima, Y., 1980b. Dynamic model of enhanced boiling heat transfer on porous surfaces – Part II. ASME Journal of Heat Transfer 102, 451–456.

O'Neill, P.S., Gottzmann, C.F., Terbot, J.W., 1972. Novel heat exchanger increases cascade cycle efficiency for natural gas liquefaction. In: Timmerhaus, K.D. (Ed.), Advances in Cryogenic Engineering, vol. 17. Plenum Press, New York, pp. 420–437.

Rao, S.M., 1997. Enhancement of flow boiling heat transfer on cylinders using interference sleeves. Ph.D. Thesis, Indian Institute of Technology Madras, Chennai, India.

Rao, S.M., Balakrishnan, A.R., 1997a. Analysis of pool boiling heat transfer over porous surfaces. Wärme und Stoffübertragung 32, 463–469.

Rao, S.M., Balakrishnan, A.R., 1997b. Enhancement of subcooled flow boiling heat transfer on cylinders using interference sleeves. Journal of Enhanced Heat Transfer 4, 203–215.

Rouhani, Z., 1969. Modified correlations for void fraction and two-phase pressure drop. AB Atomenergi Sweden, AE-RTV-841, 1/10.

Shah, M.M., 1982. Chart correlations for saturated boiling heat transfer: Equations and further study. ASHRAE Trans. 88, 185–196.

Shimada, R., Komai, J., Hirono, Y., Kumagai, S., Takeyama, T., 1991. Enhancement of boiling heat transfer in a narrow space restricted by an interference plate with holes. Experimental Thermal and Fluid Science 4, 587–593.

Tehver, J., Sui, H., Temkina, V., 1992. Heat transfer and hysteresis phenomena in boiling on porous plasma sprayed surfaces. Experimental Thermal and Fluid Science 5, 714–727.

Webb, R.L., 1994. Principles of Enhanced Heat Transfer. Wiley, New York.